



Thermal Infrared and Optical Photometry of Asteroidal Comet C/2002 CE₁₀

Tomohiko Sekiguchi^a, Seidai Miyasaka^b, Budi Dermawan^c, Thomas Mueller^d, Naruhisa Takato^{e,f}, Junichi Watanabe^e, Hermann Boehnhardt^g

^a Hokkaido University of Education, 9 Hokumon, Asahikawa, Japan

^b Tokyo Metropolitan Government, 2-8-1, Nishishinjuku, Shinjuku, Tokyo, Japan

^c Department of Astronomy, Bandung Institute of Technology, Bandung 40132, Indonesia

^d Max-Planck-Institute for Extraterrestrial Physics, Giessenbachstrasse, 85748 Garching, Germany

^e National Astronomical Observatory of Japan, 2-21-1 Osawa, Mitaka, Tokyo, Japan

^f Subaru Telescope, 650 North A'ohoku Pl., Hilo, HI, USA

^g Max-Planck-Institute for Solar System Research, Justus-von-Liebig-Weg 3, 37077 Göttingen, Germany

Abstract

C/2002 CE₁₀ is an object in a retrograde elliptical orbit with Tisserand parameter -0.853 indicating a likely origin in the Oort Cloud. It appears to be a rather inactive comet since no coma and only a very weak tail was detected during the past perihelion passage. We present multi-color optical photometry, lightcurve and thermal mid-IR observations of the asteroidal comet. With the photometric analysis in *BVRI*, the surface color is found to be redder than asteroids, corresponding to cometary nuclei and TNOs/Centaurs. The time-resolved differential photometry supports a rotation period of 8.19 ± 0.05 h. The effective diameter and the geometric albedo are 17.9 ± 0.9 km and 0.03 ± 0.01 , respectively, indicating a very dark reflectance of the surface. The dark and redder surface color of C/2002 CE₁₀ may be attribute to devolatilized material by surface aging suffered from the irradiation by cosmic rays or from impact by dust particles in the Oort Cloud. Alternatively, C/2002 CE₁₀ was formed of very dark refractory material originally like a rocky planetesimal. In both cases, this object lacks ices (on the surface at least). The dynamical and known physical characteristics of C/2002 CE₁₀ are best compatible with those of the Damocloids population in the Solar System, that appear to be exhaust cometary nucleus in Halley-type orbits. The study of physical properties of rocky Oort cloud objects may give us a key for the formation of the Oort cloud and the solar system.

© 2011 Published by Elsevier Ltd.

Keywords:

Asteroids, Asteroids surface, Comets, Comets nucleus, Infrared observations, Photometry,

1. Introduction

On February 2, 2002, the LINEAR project of the MIT Lincoln Laboratory in Socorro, USA, discovered an object approaching the Sun at about Jupiter's distance. Although of asteroidal appearance without sign of activity, it was classified as cometary object, C/2002 CE₁₀, based upon its retrograde comet-like orbit (see Table. 1). Deep imaging of the object, obtained with the Subaru telescope around the period of closest approach to Earth, revealed a short faint

Table 1. Orbital information of C/2002 CE₁₀ (orbital elements taken from M.P.E.C. 2003-R41)

a : semimajor axis	9.815 (au)
q : perihelion distance	2.047 (au)
Q : aphelion distance	17.585 (au)
e : eccentricity	0.7915
i : inclination	145.46 (°)
ω : argument of perihelion	126.19 (°)
Ω : longitude of the ascending node	147.44 (°)
M : mean anomaly	0.0609 (°)
n : mean motion	0.0320 (°/d)
Perihelion Passage	2003, June 22.10 TT
Earth Approach	2003, Sept 04.90 TT ($\Delta = 1.231$ au)
P : orbital period	30.75 (years)
T_J : Jupiter Tisserand parameter	-0.853

tail of C/2002 CE₁₀ (Takato et al. 2003). The faint tail may either be caused by very weak or by temporal cometary activity (sublimation of gas and release of embedded dust), or it may be due to a recent impact event of low, but non-zero occurrence probability. Since cometary coma activity in C/2002 CE₁₀ has not been reported so far despite deep imaging attempts using the Subaru telescope’s Prime Focus Camera: Suprime-Cam, and despite the object passed through perihelion well within the water sublimation limit, C/2002 CE₁₀ may represent a transitional object between the population classes of comets and asteroids. This paper primarily presents an analysis of the nucleus properties of this object and the properties of dust tail with the Finson-Probstein analysis and no coma activity will be analyzed in a future paper.

The criteria for classification a minor body as asteroid or as comet are appearance (coma and tail versus point-like) and orbit parameters, namely the Tisserand parameter, T_J . The parameter T_J characterizing the dynamical link of minor bodies to the gravitational disturbance by planet Jupiter (Carusi et al. 1995) is used to differentiate the Halley-type comets ($T_J < 2$) from the Jupiter-family comets ($3 > T_J > 2$) and objects with $T_J > 3$ are generally considered to be dynamically asteroidal. It is given by $T_J = \frac{a_J}{a} + 2 \left\{ \frac{a_J}{a} (1 - e^2) \right\}^{\frac{1}{2}} \cos(i)$, where a_J and a are the semi-major axis of Jupiter and the object (asteroid, comet or others) respectively, i and e are the object’s inclination and eccentricity, respectively. Recently, this classification approach is challenged by the discovery of objects of cometary appearance in asteroid-like orbits, the so called “Main Belt Comets” (MBCs), and of objects of point-like appearance in cometary orbits. Jewitt (2005) assigned Halley-type orbit asteroids and inactive comets into a new group, the “Damocloids”, named after asteroid (5335) Damocles. Meech et al. (2016) reported that Oort cloud comet C/2014 S3 (PANSTARRS) shows a very weak level of cometary activity and S-type asteroid spectra with a silicate absorption feature around 1 μm wavelength, indicating that the comet may be physically similar to an inner main belt rocky S-type asteroid.

The T_J -value of C/2002 CE₁₀ is -0.853 (Tab. 1), indicating in object in an Halley-type orbit. This result together with no coma appearance (Takato et al. 2003) suggests that C/2002 CE₁₀ might be either an extinct comet or a quasi-inert object that has been eject from the Oort Cloud, giving us a good opportunity to investigate basic physical characteristics of an Oort Cloud object. Furthermore, the results may provide insights in the surface aging of minor bodies and the link between asteroids and comets. After an outline of the observations and data reduction performed, we present results on physical properties of C/2002 CE₁₀: rotation period, axis ratio, dimension, albedo and color taxonomy. In the final section of the paper we discuss, based upon our findings, the relation of C/2002 CE₁₀ with other minor body populations in the solar system.

2. Observations and Data Reduction

C/2002 CE₁₀ was observed in September and October 2003 in the visible and thermal infrared wavelength ranges.

Table 2. Observing Geometry of C/2002 CE₁₀

Date (UT)	R_h^a (au)	Δ^b (au)	Phase Angle (deg.)	Observation Type (& band)	Telescope	sky condition
2003-Sep-06	2.20	1.23	9.8°	thermal IR (<i>N</i>)	ESO 3.6 m	photometric
2003-Oct-02	2.31	1.57	20.1°	color (<i>BVRI</i>) & lightcurve (<i>I</i>)	Kiso 1.05 m	photometric
2003-Oct-03	2.32	1.59	20.5°	lightcurve (<i>I</i>)	Kiso 1.05 m	thin clouds
2003-Oct-04	2.32	1.61	20.9°	lightcurve (<i>I</i>)	Kiso 1.05 m	thin clouds
2003-Oct-06	2.33	1.66	21.6°	lightcurve (<i>I</i>)	Kiso 1.05 m	thin clouds
2003-Oct-08	2.34	1.71	22.2°	lightcurve (<i>I</i>)	Kiso 1.05 m	thin clouds

^a R_h is the heliocentric distance.

^b Δ is the geocentric distance.

2.1. Optical Observations

The *BVRI* observations of C/2002 CE₁₀ were carried out on a photometric night, 2003-Oct-3, using the 1.05 m Schmidt telescope at the Kiso observatory, Japan. The CCD camera used has 2048 × 2048 pixels with pixel size of 24 μm and covers a field of view (fov) of 50′ × 50′. It is well-suited for time-resolved observations of Solar System objects using an adequate number of reference stars in the fov for differential photometry of moving targets. *B* and *V* exposures were taken through Johnson-type filters, *R* and *I* exposures through Cron-Cousins-type filters. The multi-color photometric observations were embedded in the series of *I*-band exposures for lightcurve sampling (i.e. *–I–I–B–I–V–I–R–I–I–* sequence) in order to follow and compensate for brightness variations due to non-spherical shape or albedo in combination with the rotation motion of the object. The photometric parameters of the telescope-instrument combination and of the atmosphere were determined by measuring various standard star fields at different airmasses. Lightcurve observations were performed between 2003-Oct-2 and 2003-Oct-8, occasionally with thin clouds. In order to minimize the fluctuation of sky conditions and scattering of lunar light by thin cloud, *I*-band filter was used. The standard calibration frames (CCD bias and flatfield exposures) were also obtained as needed. Table 2 summarizes the observing geometry, exposures types and sky conditions for the C/2002 CE₁₀ observations.

Differential photometry between C/2002 CE₁₀ and comparison stars in the fov is applied. In order to reduce the influence of possible variable stars on the photometric results, to gain a high signal-to-noise ratio, and to ensure the confidence of the measurements and a good coverage for the lightcurve analysis, we selected comparison stars according to the following criteria: (1) as many as possible, (2) as bright as possible, (3) with maximum exposure level below 40,000 ADU to stay well inside the linearity range of the CCD detector, (4) visible and measurable in the whole set of images of a single night. Daily extinction and zero-point parameters were derived from the exposures of the Landolt standard star fields and by measuring the comparison stars in the object fov. Magnitudes of comparison stars are derived per night series using photometric data of the standard stars at the same airmasses.

2.2. Thermal mid-IR Observations

Thermal observations of C/2002 CE₁₀ were carried out on 2003-Sep-6. *N*-band images were taken in service mode with the 3.6 m telescope and the TIMMI2 instrument at the La Silla site of the European Southern Observatory ESO in Chile. TIMMI2, the Thermal Infrared Multi-Mode Instrument 2 (Käufl et al., 2003) has a 240 × 320 pixel SiAs detector, and it is operated at 6.5–7.5 K. The image scale used for our observations was 0.″202 pixel^{−1} which offers a field of view of 64″ × 48″ on the sky. The *N1*-filter of the TIMMI2 instrument (with effective central wavelength of 8.6 μm) was chosen because of an expected advantageous sensitivity for the observations of C/2002 CE₁₀. The individual TIMMI2 detector integration time (DIT) was set to 20.8 milliseconds. The observations were performed as a series of 4 exposures using secondary mirror chopping and telescope nodding as follows: On target position 3 DIT read-outs were taken at two chopping positions offset in North-South direction by 10″. This chopping-integration cycle was repeated 60 times. Thereafter, the telescope was moved 10″ in East-West direction and 80 chopping-integrations were repeated as before. An exposure series of C/2002 CE₁₀ were made with a total integration time of

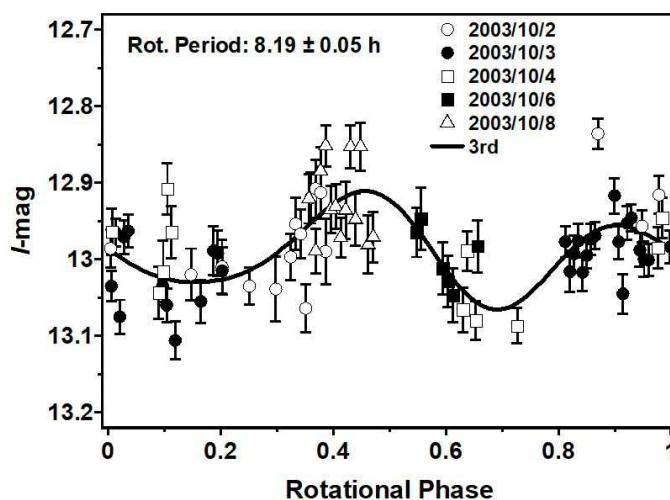


Figure 1. Fitted lightcurve of C/2002 CE₁₀ (solid line). Differential photometric observations were performed from 2003-Oct-2 to 2003-Oct-8 with the 1.05 m Schmidt telescope at the Kiso observatory in Japan.

2396.16 sec. During the observations of C/2002 CE₁₀ the sky conditions were photometric with an average seeing of 1".

The basic reduction for C/2002 CE₁₀ data makes use the TIMMI2 reduction pipeline (Relke et al. 2000, Siebenmorgen et al., 2004). The pipeline procedure automatically subtracts the pairs of “chopped” images and co-adds all the frames of the whole chopping/nodding sequence (equivalent to one exposure series). Hence, the resulting image shows 2 positive and 2 negative sub-images of C/2002 CE₁₀. The two negative ones are multiplied by -1 and all sub-images of C/2002 CE₁₀ are shifted such that the pixel positions of the brightness center in the sub-images overlap. At the end the shifted subimages are coadded to the result frame of the respective exposure series. The TIMMI2 data are flux-calibrated using observations of standard star HD156277 which were obtained during the same night applying the same filter setup and observing mode as for the observations of C/2002 CE₁₀. An airmass correction factor of 7 % is applied to compensate for the different airmasses of the standard star (airmass = 1.29) and target observations (airmass = 1.615) (see: http://www.ls.eso.org/sci/facilities/lasilla/instruments/timmi/Reports/oschuetz/Projects/T2_Extinc/TIMMI2_extinc.html and Schuetz & Sterzik (2004)). Because of the different spectral types of the standard star (K2-III) and the target (solar-type), the color correction factor is estimated to be 1–3 % in the N1 filter (Müller et al., 2004). The final result for the monochromatic flux density of C/2002 CE₁₀ at 8.7 μm is 0.50±0.05 Jy. The error accounts for the uncertainties in airmass correction, as well as for the 1.6 % stellar model uncertainty (Cohen et al., 1999) and the spectral color correction.

3. Results

3.1. Rotation period and body axis ratio

Two independent methods were used for the periodogram analysis of the *I*-filter lightcurve of C/2002 CE₁₀, e.g. Lomb’s spectral analysis (Lomb 1976) which is widely used as a standard method to calculate the power spectra of unevenly spaced time-series data, and the Window-CLEAN method (Roberts et al. 1987) which was originally developed in radio astronomy for UV-plane image synthesis. More specifically, we applied the implementation of the time series analysis by Yoshida et al. (2016) used for asteroid lightcurve data. This analysis approach was used previously to determine the rotational period of asteroid 25143 Itokawa, which was later confirmed by the Hayabusa space mission (Dermawan et al., 2002). The two highest peaks of Window-CLEAN periodograms of the C/2002 CE₁₀ lightcurve data coincide with those of Lomb-Scargle approach applied in parallel to the same dataset. The Lomb-Scargle scheme shows both peaks at significance level of 98 % (Fig. 2). A rotation period of 8.19±0.05 h is considered the most probable solution for C/2002 CE₁₀. However, other solutions for the rotation period of the object cannot completely ruled out based upon the dispersion inherent in the photometric data of C/2002 CE₁₀ (Fig. 1).

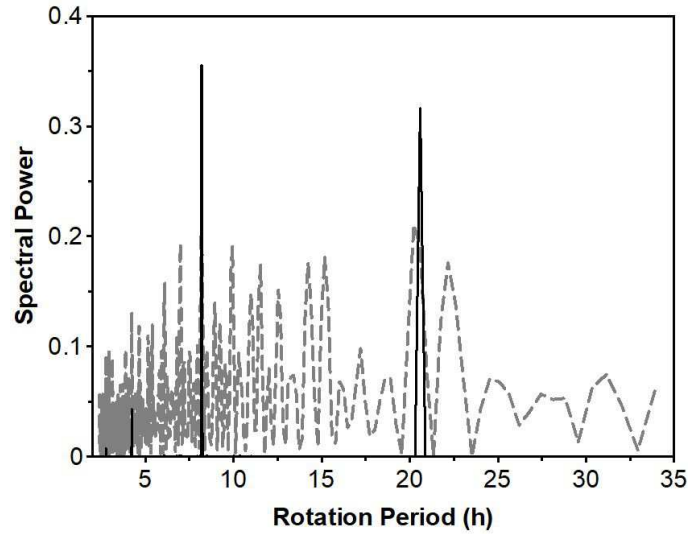


Figure 2. Analysis of the lightcurve–rotation period of C/2002 CE₁₀. The solid line shows the result for Window-CLEAN method, and the dashed-line is for Lomb-Scargle spectral analysis. The uncertainty of the rotation period was calculated considering the frequency interval (Fourier transform) of Window-CLEAN around the highest peak of the obtained spectral power, i.e. 0.04656 h. The second highest peak is located at 20.58 h. Note that the two highest peaks of Window-CLEAN coincide with those of Lomb-Scargle, and the Lomb-Scargle scheme shows both peaks with 98 % significance level.

Table 3. Colors of C/2002 CE₁₀ in magnitude

$B - V$	$V - R$	$V - I$	$V(1, 1, 0)^a$
0.734 ± 0.034	0.568 ± 0.039	1.075 ± 0.033	13.07 ± 0.07

^a $V(1, 1, 0) = H$ is the absolute magnitude in V -band

Assuming that the lightcurve of C/2002 CE₁₀ are caused by the non-spherical shape of its nucleus alone (e.g. Sekiguchi et al., 2002), a lower limit for the shape elongation, i.e. the a/b axis ratio, can be estimated as $a/b \geq 10^{0.4\Delta m} = 1.2 \pm 0.1$, where Δm is the peak-to-valley amplitude of the fitted lightcurve (in magnitude).

3.2. Absolute Magnitude and Spectral Colors

For the determination of the absolute magnitude of C/2002 CE₁₀ the analysis approach based upon the HG system (Bowell et al., 1989) of the International Astronomical Union IAU is chosen:

$$V(1, 1, \alpha) = V(1, 1, 0) - \log \left[(1 - G)\Phi_1(\alpha) + G\Phi_2(\alpha) \right]^{\frac{2}{5}}, \quad (1)$$

where $V(1, 1, \alpha)$ is the V -band magnitude reduced to unity Sun and Earth distances $R_h = \Delta = 1$ au at phase angle α , and $V(1, 1, 0)$ is the absolute magnitude H . G represents the slope parameter in V -band. Φ_1 and Φ_2 are describing the phase function and are considered filter-independent. Since for C/2002 CE₁₀ the phase angle coverage of our observations is not sufficient, we applied a predetermined values of 0.15 as a default slope parameter G (e.g. Bowell et al., 1989). The estimated absolute magnitude of C/2002 CE₁₀ in V -band is $H = 13.08 \pm 0.07$ mag. This result is used together with the thermal flux of the object in order to constrain the size and albedo of C/2002 CE₁₀ - see next section.

The photometric results of C/2002 CE₁₀ are illustrated in terms of colors $B - V$, $V - R$, $V - I$ (see Tab. 3) that are representing coarse measures of the global surface taxonomy of the object. In Fig. 3 the three broadband colors of C/2002 CE₁₀ (marked by circle with error bars) are plotted together with the colors of asteroids (colored squares), comets, Transneptunian Objects (TNOs) and Centaurs (colored triangles). The surface taxonomy of C/2002 CE₁₀ is

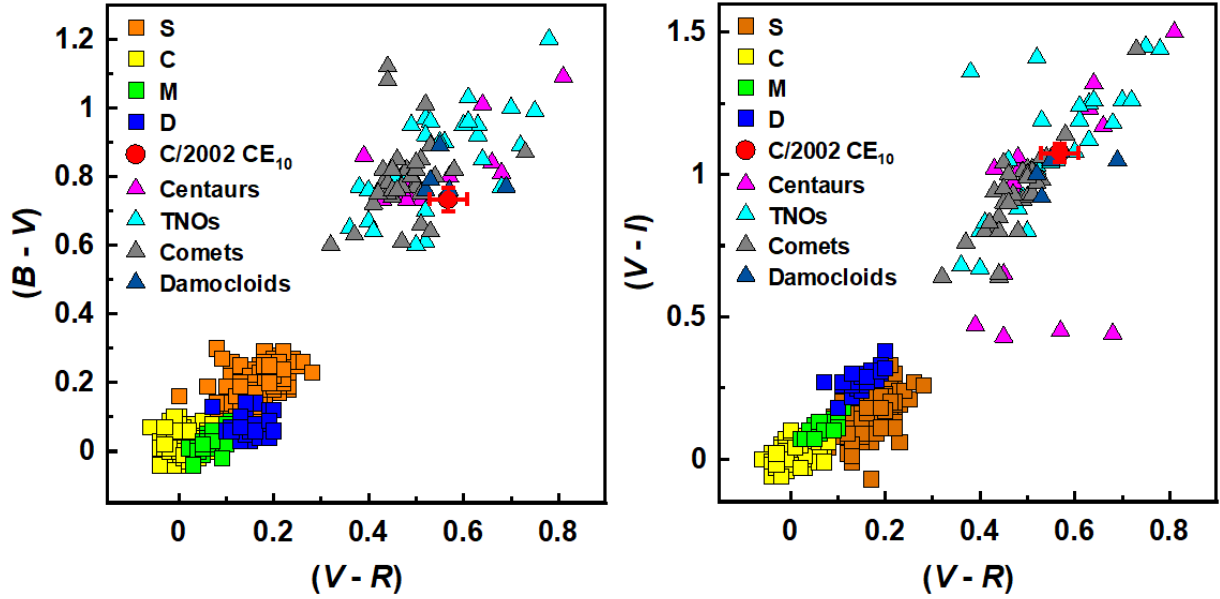


Figure 3. Color-color diagrams of different minor body groups including C/2002 CE₁₀. The comet and Damocloids data were taken from Abell et al. (2003), Campins et al. (2006), Doressoundiram et al. (2007), Hicks and Bauer (2007), Jewitt et al. (2009), Lamy and Toth (2009), Jewitt (2015). The square symbols in Fig. 3 denote the taxonomy ranges of S-type, C-type, M-type and D-type asteroids, respectively, from the eight-colors asteroid survey data by Zellner et al. (1985) and from NASA's Planetary Data System: Small Bodies Node (<https://pds.nasa.gov/>). The colors for TNOs are taken from Boehnhardt et al. (2003), Sheppard and Jewitt (2002), Mueller et al. (2004), Peixinho et al. (2004), Doressoundiram et al. (2007), Sheppard (2010), Perna et al. (2013) while the Centaurs data are taken from the papers of Gutierrez et al. (2001), Bauer et al. (2003), Doressoundiram et al. (2007), Perna et al. (2013), Jewitt (2015).

clearly redder than and much beyond the colors of the different asteroid types. It falls well in the middle of the range for TNOs, Centaurs, and cometary nuclei.

3.3. Thermal mid-IR

The thermal IR count rates of C/2002 CE₁₀ and of the standard star were measured from the respective *N*-band images using the aperture photometry method. Using the determined thermal flux of the standard star, the *N*-band flux of C/2002 CE₁₀ was determined to be 0.50 ± 0.05 Jy. The error accounts for measurement uncertainties, the uncertainties in airmass correction, as well as for the 1.6 % stellar model uncertainty (Cohen et al. 1999) and in the color correction.

The thermal flux density of mid-IR radiation is given by

$$S_{\nu} = \pi \varepsilon \left(\frac{r_N}{\Delta} \right)^2 B_{\nu}(T), \quad (2)$$

where r_N is the radius of C/2002 CE₁₀ (in m), $\varepsilon = 0.9$ (Lebofsky et al., 1986) is the infrared emissivity, Δ is the geocentric distance (in m) and $B_{\nu}(T)$ is the Planck function for the effective surface temperature T . The effective surface temperature of minor bodies is determined from the energy balance at the surface (e.g. Lebofsky & Spencer, 1989). However, it also implies knowledge or an estimation of the surface temperature of the object. Since by measurements of a single thermal filter band, the surface temperature distribution of a minor body cannot be estimated, a thermal model approximation is used instead. Usually, this approach has to adopt additional values for in principle unconstrained parameters like the chemical composition, material distribution (albedo map), emissivity, density (and porosity), heat conductivity and heat capacity of the surface materials, of the rotation period and the orientation of the rotation axis with respect to the Sun.

For our analysis of the TIMMI2 data of C/2002 CE₁₀, we applied the so called NEATM model (Near Earth Asteroid Thermal Model; Harris, 1998) that is adopted to a specific object group. The NEATM is modified from the

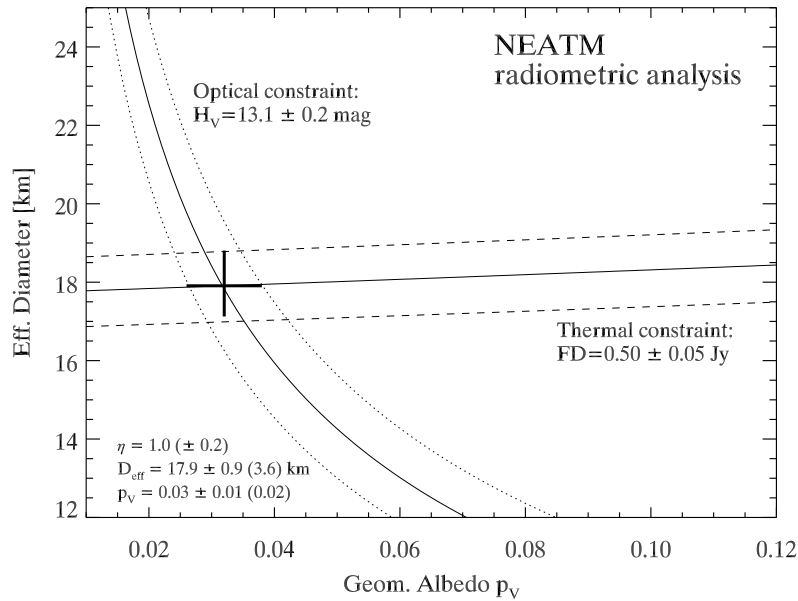


Figure 4. Size and albedo relationship of C/2002 CE₁₀. The figure shows a graphical representation of the radiometric method: The solid (with error) curve represents the “optical constraint”, based on the H -magnitude. The almost horizontal curve (with error) represents the “thermal constraint” coming from the TIMMI2 measurements. The thermal flux is tightly connected to the size of the object.

Standard Thermal Model (STM) of Lebofsky et al. (1986) which is usually used for minor body applications (e.g. Sekiguchi et al., 2003).

Fernández et al. (2013) and Licandro et al. (2016) show that comets as well as asteroids in cometary orbits (including Damocloids) present beaming parameters of $\eta = 1.0 \pm 0.2$. The bond albedo A and geometric albedo are related by $A = p q = p_V q$, where p and p_V are the bolometric geometric albedo and the geometric albedo in V -band, respectively. q is the bolometric phase integral which in the H - G system is derived from the slope parameter G , via $q = 0.290 + 0.684 G$ (Bowell et al., 1989).

The absolute magnitude H , geometric albedo p_V and diameter D (km) for asteroids are related by (e.g., Fowler & Chillemi, 1986)

$$\log_{10} D = 3.1236 - 0.2 H - 0.5 \log_{10}(p_V), \quad (3)$$

Fig. 4 shows the diameter versus the geometric albedo relationship for C/2002 CE₁₀ using the measurement results in the visible and thermal wavelength range (including uncertainties). In the figure the optical constraint, representing the H magnitude of the object in Eq. (3), is shown as decreasing curves. The thermal constraint representing the IR flux of the object is an almost horizontal curve (plus parallel lines indicating the uncertainty ranges). The simultaneous solution of thermal and optical constraint in Eq. 2 and Eq. 3, respectively, is the the intersection of the respective curves. Thus, the best estimate for the radius r and albedo p_V of C/2002 CE₁₀ is found to be: $r = 17.9 \pm 0.9$ km, $p_V = 0.03 \pm 0.01$.

4. Discussion

The dynamical and physical characteristics of C/2002 CE₁₀ suggest several similarities with minor bodies from the outer solar system: very low Tisserand parameter, red color, low albedo. The presence of a tail in 2002 indicates a link to the comets population, although it is not known whether it is driven by repetitive and extended periods of cometary activity due to ice sublimation, or by a rare and singular activity event, caused for instance by an impact.

C/2002 CE₁₀ is in an orbit that crosses the orbital distances of the giant planet. For this reason it is likely in a transitional orbit state, since it is exposed to encounters with the gas giants in the planetary system and thus to gravitational scattering in the future and it was so in the past. Various reservoirs of minor bodies can be considered as the original home region of C/2002 CE₁₀: The Kuiper Belt and the Oort Cloud as main reservoirs for the short-periodic and long-periodic comets, respectively. While the known physical characteristics (size, color, albedo, axis ratio) are not very conclusive (whether the object has to be seen as short-periodic comet coming from the Kuiper Belt or as long-periodic comet from the Oort Cloud), the Tisserand parameter and the high inclination orbit of C/2002 CE₁₀ clearly favor an origin as for the long-periodic comets.

The Oort cloud objects ($a \sim 10,000$ au) are thought to have originally formed in the giant planet region. As soon as the giant planets had formed, they were removed from that region in the formation disk of the solar system by gravitational interaction with these planets and got stranded and dynamically thermalized in the Oort Cloud (e.g. Weissman et al. 2002). Inward scattering by masses in the closer and further distance of the solar system in the galaxy brings Oort Cloud comets back into the range of the planets.

The non-detection or the very weak level of cometary activity during the perihelion arc of the orbit that C/2002 CE₁₀ passed through in 2002 to 2003 with solar distances well within the water sublimation limit, may indicate a rather exhausted state of the nucleus activity. So, C/2002 CE₁₀ can be seen as a member of the group of Damocloids. Its surface color is in good agreement with the average color of Damocloids: $B - V = 0.80 \pm 0.02$, $V - R = 0.51 \pm 0.02$, $R - I = 0.47 \pm 0.02$, $B - R = 1.31 \pm 0.02$ (Jewitt, 2015). Jewitt (2005) reported the lack of ultrared matter in Damocloids as for instance seen in the population of the dynamically cold Classical Disk Objects in the Kuiper Belt (Hainaut et al., 2012). The estimated size of C/2002 CE₁₀ of 17.9 ± 0.9 km is in the middle (a little bigger) of the size range obtained for Damocloids using WISE data (Licandro et al., 2016). The derived radiometric albedo of 0.03 ± 0.01 (or 0.02 if the an η range 0.8–1.2 is considered) agrees with the albedo range of 0.02–0.06 for cometary nuclei (see for instance Campins and Fernández 2002, Lamy et al. 2004). It is close to the mean visible geometric albedo of 0.04 for Jupiter-family comets obtained by Fernández et al. (2013), and also close to the mean geometric albedo of 0.05 ± 0.02 found by Licandro et al. (2016) for asteroids in cometary orbits. On the other side, the albedo of C/2002 CE₁₀ represents the lower limit of the albedos found for Kuiper Belt objects (Lacerda et al. 2014) and is clearly below that of several dynamical sub-populations therein. However, its surface colors would comply with these, while its retrograde orbit may not be easily accomplished through gravitational scattering from that region by a giant planet.

Comparing C/2002 CE₁₀ with short/long-periodic comets requires an explanation of its low level or absence of activity during perihelion: Exhaustion of the sublimating ices or coverage of the surface by thick layers of regolith from previous activity cycles that may prevent the solar heat wave to reach the still present ice reservoirs underneath. The fraction of active regions on cometary surfaces with volatile ices is generally small and most of the activity originates from sub-surface layers (e.g. Keller et al. 1986). Recently, the ROSETTA mission has obtained a significant number of detailed images of 67P/Churyumov-Gerasimenko that reveal a lack of distinct active region with exposed fresh ice chunks (Thomas et al., 2015). The mission has also demonstrated the existence of meter-thick regolith on the nucleus surface that represents ballistic fall-back material from cometary activity.

The "Grand Tack" model showed that the giant planets scattered inner solar system material outward during their inward migration, and vice versa, they scattered icy planetesimals into the inner solar system during their outward migration (Walsh et al, 2011). The surface color of C/2002 CE₁₀ is much redder than that of asteroids and perhaps its extremely low Tisserand parameter and retrograde orbit which make an origin of the object in the main asteroid belt unlikely. However, a scenario of an inward scattered and stranded object from the outer solar system may be a valid explanation for C/2002 CE₁₀.

Recently inactive minor body with hyperbolic eccentricity, 1I/2017 U1 ('Oumuamua) was discovered and its physical properties are studied (Meech et al, 2017). It can be either from interstellar originally or from other planetary systems, or from our Oort cloud as a result of multiple scattering due to stellar encounters. The investigation of the evolution of the Oort cloud may give a hint to understand the relationship among such outer rocky minor bodies.

Acknowledgments

We are grateful for the recommendations and suggestions to this manuscript made by Olivier Hainaut, Henry Hsieh and one anonymous reviewer. This work is based on observations collected at the European Organization for Astronomical Research in the Southern Hemisphere ESO under programme 60.A-9126(F).

References

- [1] Abell, P. A., Fernández, Y. R., Pravec, P., et al. 2005, *ICARUS*, 179, 174
- [2] Bauer, J. M., Meech, K. J., Fernández, Y. R., et al. 2003, *ICARUS*, 166, 195
- [3] Boehnhardt, H., Barucci, A., Delsanti, A. et al. 2003, *Earth Moon & Planets*, 92, 145
- [4] Bowell, E., Hapke, B., Domingue, D., et al. 1989, In *Asteroids II*, ed. Binzel, R., Gehrels, T. & Matthews, M. S. (Tucson: Univ. Arizona Press), 524
- [5] Campins, H., & Fernández, Y. 2002, *Earth Moon & Planets*, 89, 117
- [6] Campins, H., Ziffer, J., Licandro, J., et al. 2006, *AJ*, 132, 1346
- [7] Carusi, A., Kresak, L., & Valsecchi, G. B. 1995, *Earth Moon & Planets*, 68, 71
- [8] Cohen, M., Walker, R. G., Carter, B., et al. 1999, *AJ*, 117, 1864
- [9] Dermawan, B., Nakamura, T., Fukushima, H., et al. 2002, *PASJ*, 54, 635
- [10] Doressoundiram, A., Peixinho, N., Moullet, A., et al. 2007, *AJ*, 134, 2186
- [11] Fernández, Y. R., Kelley, M. S., Lamy, P. L., et al. 2013, *Icarus*, 226, 1138
- [12] Fernández, Y. R., Jewitt, D. C., & Sheppard, S. S. 2001, *ApJL*, 553, L197
- [13] Fowler, J. W. & Chillemi, J. R., 1986, In *IRAS Asteroid and Comet Survey*, ed. Matson, D. L. (JPL: IPAC), 6-1
- [14] Gutiérrez, P. J., Ortiz, J. L., Alexandrino, E., Roos-Serote, M., & Doressoundiram, A. 2001, *A&A*, 371, L1
- [15] Hainaut, O. R., Boehnhardt, H., & Protospapa, S. 2012, *A&A*, 546, A115
- [16] Harris, A. W. 1998, *Icarus*, 131, 291
- [17] Hicks, M. D., & Bauer, J. M. 2007, *APJL*, 662, L47
- [18] Jewitt, D., 2005, *AJ*, 129, 530
- [19] Jewitt, D. 2009, *AJ*, 137, 4296
- [20] Jewitt, D. 2015, *AJ*, 150, 201
- [21] Keller, H. U., Arpigny, C., Barbieri, C. et al. 1986, *Nature*, 321, 320
- [22] Käufel, H., Sterzik, M. F., Siebenmorgen, R. et al. 2003, *Proceedings SPIE*, 4841, 117
- [23] Lacerda, P., Fornasier, S., Lellouch, E. et al. 2014, *ApJ*, 793, L2
- [24] Lamy, P. L., Toth, I., Fernández, Y. R., & Weaver, H. A. 2004, *Comets II*, 223
- [25] Lamy, P. L., Toth, I., Weaver, H. A., A'Hearn, M. F., & Jorda, L. 2009, *A&A*, 508, 1045
- [26] Lebofsky, L. A., Sykes, M. V., Tedesco, E. F., et al., 1986, *Icarus*, 68, 239
- [27] Lebofsky, L. & Spencer, J., 1989, In *Asteroids II*, ed. Binzel, R., Gehrels, T. & Matthews M. S. (Tucson: Univ. Arizona Press), 128
- [28] Licandro, J., Alí-Lagoa, V., Tancredi, G., & Fernández, Y. 2016, *A&A*, 585, A9
- [29] Lomb, N. R. 1976, *APSS*, 39, 447
- [30] Meech, K. J., Yang, B., Kleyna, J., et al. 2016, *Science Advances*, 2, e1600038
- [31] Meech, K. J., Weryk, R., Micheli, M., et al. 2017, *Nature*, in press.
- [32] Mueller, B. E. A., Hergenrother, C. W., Samarasinha, N. H., Campins, H., & McCarthy, D. W. 2004, *ICARUS*, 171, 506
- [33] Müller, T. G., Sterzik, M. F., Schütz, O., Pravec, P., & Siebenmorgen, R. 2004, *A&A*, 424, 1075
- [34] Peixinho, N., Boehnhardt, H., Belskaya, I., et al. 2004, *ICARUS*, 170, 153
- [35] Perna, D., Dotto, E., Barucci, M. A., et al. 2013, *A&A*, 554, A49
- [36] Relke, H., Sperl, M., Hron, J., et al. 2000, *SPIE*, 4009, 440
- [37] Roberts, D. H., Lehar, J., & Dreher, J. W. 1987, *AJ*, 93, 968
- [38] Schütz, O., & Sterzik, M. 2005, *High Resolution Infrared Spectroscopy in Astronomy*, 104
- [39] Sekiguchi, T., Boehnhardt, H., Hainaut, O. R., & Delahodde, C. E. 2002, *A&A*, 385, 281
- [40] Sekiguchi, T., Abe, M., Boehnhardt, H., Dermawan, B., Hainaut, O. R., & Hasegawa, S. 2003, *A&A*, 397, 325
- [41] Sheppard, S. S., & Jewitt, D. C. 2002, *AJ*, 124, 1757
- [42] Sheppard, S. S. 2010, *AJ*, 139, 1394
- [43] Siebenmorgen, R., Krügel, E., & Spoon, H. W. W. 2004, *A&A*, 414, 123
- [44] Takato, N., Sekiguchi, T., & Watanabe, J. 2003, *IAUC*, 8193, 1
- [45] Thomas, N., Sierks, H., Barbieri, C., et al. 2015, *Science*, 347, aaa0440
- [46] Walsh, K. J., Morbidelli, A., Raymond, S. N., O'Brien, D. P., & Mandell, A. M. 2011, *Nature*, 475, 206
- [47] Weissman, P. R., Bottke, W. F., & Levison, H. F., 2002, In *it Asteroids III*, ed. Bottke Jr., W. F., Cellino, A., Paolicchi, P. and Binzel, R. P., (Tucson: Univ. Arizona Press), 669
- [48] Yoshida, F., Ito, T., Dermawan, B., et al. 2016, *ICARUS*, 269, 15
- [49] Zellner, B. Tholen, D. J., & Tedesco, E. F., 1985, *ICARUS*, 61, 355